ANALYSIS OF OPTICAL NETWORKS WITH HETEROGENEOUS GROOMING ARCHITECTURES *

R. Srinivasan
Department of Electrical and Computer Engineering
University of Arizona, Tucson, AZ 85721
srini@ece.arizona.edu

Arun K. Somani
Dependable Computing & Networking Laboratory
Department of Electrical and Computer Engineering
Iowa State University, Ames, IA 50011
arun@iastate.edu

Abstract Traffic grooming in optical networks employing Wavelength Division Multiplexing (WDM) has gained prominence due to the prevailing disparity between the user requirement and the capacity of a wavelength. Nodes in an optical network get upgraded to the latest grooming technology slowly with time. Hence, WDM grooming networks are expected to employ heterogeneous grooming architectures. In this paper, we develop an analytical model to evaluate the blocking performance of WDM grooming networks with heterogeneous grooming capabilities. We demonstrate the accuracy of the analytical model by comparing the analytical results with that of the simulation. We observe that analytical models with and without the precise knowledge on the grooming architectures predict similar performance. The proposed analytical model can be employed by resource placement algorithms that identify a set of nodes and links that need to be upgraded when the resources are limited.

Keywords: Optical networks, WDM/TDM switching, performance modeling, heterogeneous grooming architectures, blocking probability

*The research reported in this paper is funded in part by the National Science Foundation under grant ANI-9973102, Defense Advanced Research Projects Agency under contract N66001-00-1-8949, and David C. Nicholas Professorship Fund at Iowa State University.

1. Introduction

Optical networks employing Wavelength Division Multiplexing (WDM) divide the fiber bandwidth into multiple wavelengths. The current transmission capacity on each wavelength is around peak electronic speed of 10 Gbps (OC-192) and is likely to increase to 40 Gbps (OC-768). However, the user traffic requirements are in the range of 155 Mbps (OC-3) to 622 Mbps (OC-12) and rarely in the range of a few gigabits per second. Such a vast difference in the granularity of bandwidth requirement of users versus the bandwidth offered by a network has necessitated efficient sharing of a wavelength capacity by multiple users, referred to as *traffic grooming*.

One approach to achieve traffic grooming is to divide the capacity available on a wavelength into multiple time slots. Users could be assigned one or more time slots on a wavelength depending on the requirement. Nodes in grooming networks could employ wavelength converters and/or time slot interchangers that convert signals from one wavelength and/or time slot to another. Nodes can therefore have different levels of grooming capability. For example, a node might employ time slot interchange but not wavelength conversion. Such nodes are referred to as wavelength-level grooming nodes as connections can be switched only within a wavelength. Similarly some other node might implement wavelength conversion but not time slot interchangers (eg. photonic slot routing nodes with wavelength conversion), referred to as time slot level grooming node. A node employing both wavelength conversion and time slot interchange is referred to as full-grooming node.

Employing sophisticated grooming capabilities at all nodes would definitely improve the performance of a network, however, it is an expensive proposition. Financial constraints limit the network upgrade procedure to enhancing the capability of only a few nodes or increasing the capacity of only a few links depending on the traffic flowing through them. Hence, optical grooming networks are expected to employ heterogeneous switching architectures. As simulations take a large amount of time to yield results, analytical models are typically employed to evaluate network performance. Therefore, analytical models must be able to compute network performance with nodes in the network having heterogeneous switching architectures.

Wide-area optical networks are expected to be circuit-switched in nature as the optical processing technology is not mature to achieve run-time routing decisions. The performance of circuit-switched networks are primarily computed as the ratio of number of calls rejected in the network to the total number of calls, referred to as *blocking probability*. Several analytical models have been proposed in the literature for the computation of blocking probability in optical networks, specifically on: (a) performance of wavelength-routed WDM network and benefits of wavelength conversion [1, 2, 3, 4]; (b) sparse-wavelength conversion where only a few nodes in the network employ full-wavelength conversion [10]; (d) limited-range wavelength conversion where a wavelength could be converted to a set of but not all wavelengths, employed at every node in the network [6, 12]; (e) multi-fiber wavelength-routed networks [5, 13]; (f) WDM/TDM networks [14, 8]. There has not been any work that targets heterogeneous WDM grooming network for analysis.

In this paper, we develop an analytical model to evaluate the blocking probability in WDM grooming networks with heterogeneous grooming capabilities. The remainder of the paper is organized as follows: Section 2 describes the network model. The analytical model is developed in Section 3. Details on the simulation methodology of WDM grooming networks are presented in Section 4. Performance results and comparison of analytical model to simulation results are shown in Section 5. Section 6 concludes the paper.

2. Network model

We consider a WDM grooming network with nodes employing heterogeneous switching architecture. The nodes in the network are connected using links. Each link is assumed to carry F fibers, each fiber carrying W wavelengths. Each wavelength is divided into frames which are further sub-divided into T time slots. Every slot within a frame is denoted by a 4-tuple, (l, f, w, t), where $1 \leq l \leq L$, $1 \leq f \leq F$, $1 \leq w \leq W$, and $1 \leq t \leq T$. For example, the tuple $(1, 1, 2, 1)$ (read from right to left) denotes first time slot in a frame on the second wavelength of the first fiber on the first link. A *channel* on a link is defined as a collection of a particular time slot across successive frames. Hence, the number of channels in a link is the same as the number of slots in a frame, $F \times W \times T$. Each channel is also represented by a 4-tuple, (l, f, w, t), similar to the representation of a slot.

2.1. Node architecture

A WDM grooming network with heterogeneous network architecture is modeled as a Trunk Switched Network (TSN) [8]. A TSN is a two-level network model in which every link in the network is viewed as multiple channels.

A node in a TSN groups the channels with similar characteristics in a link into groups called *trunks*. Fig. 1 shows the node architecture in a TSN. The node in the figure is assumed to have three links attached to it and views each link as a set of four trunks. The trunks are first de-multiplexed from the link. The trunks from different links are then sent to their respective trunk switches where the channels are switched. We impose trunk-continuity constraint at a node, i.e., a channel in a trunk on a link can be switched to a channel that falls within the same trunk on another link. Such a restriction stems from the architectural point of view. The complexity of having a switch architecture that could fully permute all the channels across all the links is very high. Therefore, switch design for the near future are likely to be based on simple architectures that would work on a restricted set of channels from every incoming link. In this paper, it is assumed that a full-permutation switch is employed for every trunk in a node, i.e., a free channel of a trunk at the input of the switch can be switched to any free channel of the same trunk at its output.

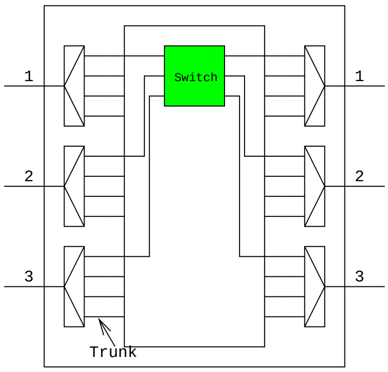

Figure 1. Node architecture in a Trunk Switched Network.

A TSN is said to be *homogeneous* if the collection of channels that constitute a trunk at a node is the same for all the nodes in the network. Otherwise, it is said to be *heterogeneous*. In this paper, we consider nodes with different grooming architectures, hence a heterogeneous TSN.

A node i in the network views a link connected to it as a set of K_i trunks with S_i channels in them. Let χ_{ix} denote the channels on a link that fall within trunk x at Node i. Let Θ_{xy}^{ij} denote the channels on link (i, j) that fall within trunk x at Node i and trunk y at Node j, i.e., $\Theta_{xy}^{ij} = \chi_{ix} \cap \chi_{jy}$. The group of channels that fall within a set Θ_{xy}^{ij} is referred to as a *sub-trunk*.

A channel on a link is said to be *busy* if it is allocated for a connection. Otherwise, it is said to be free. A trunk at a node is said to be *free* if there is atleast one free channel in the trunk. A trunk x at a node d is said to be available on a path from source s, if a connection from s to d could be established such that it terminates at node d at trunk x. Calls arriving in the network request for a connection to be established from a source to destination. The connection establishment involves selection of a path and assigning channels on the path such that the channel on one link can be switched to the successive link on the path by the node connecting the links. As every node employs full-permutation switching within a trunk, channel assignment on a chosen path is equivalent of sub-trunk assignment on the links. Any free channel within the assigned sub-trunk could be assigned for the connection.

2.2. Example

Consider a WDM grooming network where every link has three fiber, three wavelengths per fiber and two time slots per wavelength ($F = 3$, $W = 3$, $T = 2$). Figure 2 shows the eighteen channels that are available on a link. The shapes of the figures represent the time slots, the shades of the shapes represent wavelengths, and the number of shapes of a certain shade represents the number of fibers.

Figure 2. Representation of eighteen channels in a link having three fibers, three wavelengths per fiber, and two time slots per wavelength. Shapes represent time slots, shades represent wavelengths, number of shapes of a certain shade represents the number fibers.

If time slot interchange and wavelength conversion are not permitted, a node i views a link ℓ as WT trunks where each wavelength and time slot combination forms a trunk, i.e., $\chi^i_{\ell,(w,t)} = \{(l, f, w, t)|1 \leq f \leq F\}$, where $1 \leq w \leq W$ and $1 \leq t \leq T$. Every trunk has F channels as shown in Figure. 3(a).

If time slot interchange is permitted, but not wavelength conversion, a node i views a link ℓ as W trunks where each wavelength forms a trunk, i.e., $\chi^i_{\ell,w} = \{(l, f, w, t)|1 \leq t \leq T \;\; and \; 1 \leq f \leq F\}$, where $1 \leq w \leq W$. Every trunk has FT channels as shown in Fig. 3(b).

If full-wavelength conversion is permitted, but not time slot interchange, then for a given link l, a time slot on all the wavelengths can be grouped to form a trunk, i.e., $\chi^i_{\ell,t} = \{(l, f, w, t)|1 \leq w \leq W \; and \; 1 \leq f \leq F\}$, where $1 \leq t \leq T$. Every trunk has has FW channels as shown in Fig. 3(c).

If both full-wavelength conversion and time slot interchange are permitted, then the entire link is treated as one trunk with FWT channels, as shown in Fig. 3(d).

3. Analysis

The analytical model for evaluating the blocking performance is developed with the following assumptions: (1) The call arrival at every node follows a Poisson process with rate λ_n. The holding time of a call is exponentially distributed with unit mean. The choice of these specific distributions for traffic is to keep the analysis tractable; (2) A call arriving at a node is equally likely to have any other node in the network as its destination; (3) The path selection is pre-determined (fixed-path routing), eg: shortest-path. The sub-trunk assignment on a chosen path is assumed to be randomly chosen from the set of possible trunk assignments at every node; (4) A call is assigned a channel

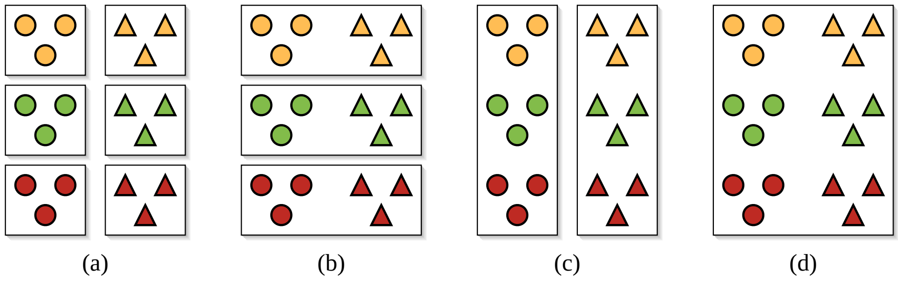

Figure 3. Possible grouping of channels in a link as trunks. (a) Wavelength-Time slot trunk (b) Wavelength trunk; (c) Time slot trunk; and (d) Link is a trunk.

randomly from a set of available channels in a sub-trunk on a link; and (5) Blocked calls are not re-attempted.

Consider a z-link path model as shown in Fig. 4. Let $P_z(T_f)$ denote the probability of T_f trunks being available on a z-link path as viewed by the last node on the path[1] (node z). The definition of the trunk is as viewed by the node denoted by the suffix for P. $P_z(T_f = 0)$ denotes the blocking probability over the z-link path.

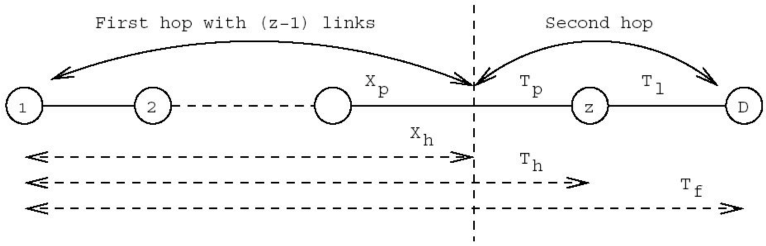

Figure 4. A z-link path.

Let $P_z(T_f, T_l)$ denote the probability of T_f trunks being available on a z-link path with T_l trunks free on the last link. It can be seen that the last link should have at-least T_f trunks free, therefore $T_l \geq T_f$. $P_z(T_f)$ can then be written as:

$$P_z(T_f) = \sum_{T_l=T_f}^{K_z} P_z(T_f, T_l) \tag{1}$$

where K_z denotes the number trunks in the link as viewed by node z.

A z-link path is analyzed as a two-hop path by considering the first $z-1$ links as the first hop and the last two links as the second hop, as shown in Fig. 4. Let X_h and X_p denote the number of trunks available on the first hop and that which are free on the last link of the first hop (link $z-1$), respectively, as viewed by the last node on the first hop (node $z-1$). Let T_h and T_p denote the number of trunks available on the first hop and number of trunks free on the last link of the first hop as seen by the node in the second hop (node z), respectively. $P_z(T_f, T_l)$ can then be recursively computed as:

$$\begin{aligned} P_z(T_f, T_l) = & \sum_{X_h=0}^{K_{z-1}} \sum_{X_p=X_h}^{K_{z-1}} \sum_{T_h=T_f}^{K_z} \sum_{T_p=X_h}^{K_z} \\ & P_{z-1}(X_h, X_p)\, P_{z,z-1}(T_h, T_p | X_h, X_p) \\ & P_z(T_f, T_l | T_h, T_p) \end{aligned} \tag{2}$$

where $P_z(T_f, T_l|T_h, T_p)$ denotes the probability of T_f trunks being available on the second hop with T_l trunks free on the last link of the second hop given that T_h trunks are available on the first hop with T_p trunks free at the input to the node on the second hop. $P_{z,z-1}(T_h, T_p|X_h, X_p)$ denotes the probability that the number of trunks available on the first hop and number of trunks free on the last link of the first hop as viewed by the node in the second hop (node z) are T_h and T_p, respectively, given that the trunk availability as viewed by the last node (node $z-1$) on the first hop are X_h and X_p, respectively. For homogeneous TSNs, for any two successive nodes $z-1$ and z on a path $P_{z,z-1}(T_h, T_p|X_h, X_p)$ is defined as:

$$P_{z,z-1}(T_h, T_p|X_h, X_p) = \begin{cases} 1 & \text{if } T_h = X_h \text{ and } T_p = X_p \\ 0 & \text{otherwise} \end{cases} \tag{3}$$

For a homogeneous TSN, Eqn. (2), therefore, reduces to:

$$P_z(T_f, T_l) = \sum_{T_h=T_f}^{K} \sum_{T_p=T_h}^{K} P_{z-1}(T_h, T_p)\, P_z(T_f, T_l|T_h, T_p) \tag{4}$$

where K denotes the number of trunks in a link as viewed by the nodes in the network. The computation of this probability for heterogeneous switching architectures is described in Section 3.1.

The starting point of the recursion, for $z = 1$, is defined as:

$$P_1(T_f, T_l) \;=\; \begin{cases} P(T_l) & \text{if } T_f = T_l \\ 0 & \text{otherwise} \end{cases} \tag{5}$$

where $P(T_l)$ denotes the probability of T_l trunks being free on a link.

$P_z(T_f, T_l|T_h, T_p)$ is computed by conditioning on the number of trunks free on the last link as viewed by node z. From this point on, we concentrate on the second hop, which is a two-link path. The definition of trunk will be assumed to be as the one viewed by the intermediate node in the two-link path.

$P_z(T_f, T_l|T_h, T_p)$ is computed as:

$$P_z(T_f, T_l|T_h, T_p) = \begin{cases} P_z(T_f|T_h, T_p, T_l)\ P_z(T_l|T_h, T_p) \\ \qquad \text{if } T_h \geq T_f \\ \\ 0 \quad \text{otherwise} \end{cases} \tag{6}$$

where $P_z(T_l|T_h, T_p)$ denotes the probability of T_l trunks being free on the last link given that T_h trunks are available on the first hop with T_p trunks free on the last link of the first hop as viewed by node z. The number of trunks free on the last link depends on the number of trunks free on the previous links. If the correlation of traffic on a link is assumed to be only due to its previous link, then it is referred to as the *Markovian correlation*. With the assumption of Markovian correlation, $P_z(T_l|T_h, T_p)$ can be reduced to $P_z(T_l|T_p)$. Hence, Eqn. (6) can be written as:

$$P_z(T_f, T_l|T_h, T_p) = \begin{cases} P_z(T_f|T_h, T_p, T_l)\ P_z(T_l|T_p) \\ \qquad \text{if } T_h \geq T_f \\ \\ 0 \quad \text{otherwise} \end{cases} \tag{7}$$

$P_z(T_f|T_h, T_p, T_l)$ denotes the probability that T_f trunks are available on the two-hop path given that T_l trunks are free on the last link and T_h trunks are available on the first hop with T_p trunks free on the last link of the first hop. It is to be noted that the trunks are defined with respect to the intermediate node in the second hop, node z in this case. With the assumption of full-permutation trunk switches employed at every node, the above probability is obtained as:

$$P_z(T_f|T_h, T_p, T_l) = \frac{\binom{T_h}{T_f}\binom{K_z - T_h}{T_l - T_f}}{\binom{K_z}{T_l}} \tag{8}$$

The probabilities $P_z(T_l|T_p)$ and $P_z(T_l)$ are computed using a two-link model as described in [8]. The details on the computation of these probabilities are omitted in this paper due to space constraints.

3.1. Mapping of trunk proabilities for heterogeneous switch architectures

In order to analyze networks with heterogeneous node architectures, the mapping of the trunk distributions from one node architecture to the other has to be computed.

Consider the intermediate link of a two-hop path connected by two nodes with different switching architectures as shown in Fig. 5.

The first node views the link as K_1 trunks with S_1 channels per trunk while the second node views the link as K_2 trunks with S_2 channels per trunk. Let

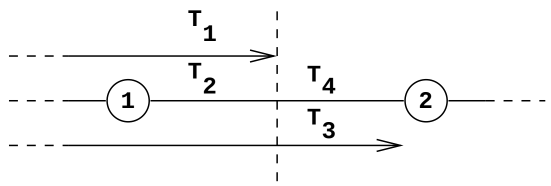

Figure 5. Trunk distribution of a link as viewed by two nodes with different switching architectures.

T_1 denote the number of available trunks on the first hop with T_2 trunks free on the last link (the link connecting nodes 1 and 2) of the first hop as viewed by node 1. Let T_3 denote the number of available trunks on the first hop and T_4 denote the number of free trunks on the last link of the first hop (the hop ends with link connecting nodes 1 and 2) as viewed by node 2. Let f_2 denote the number of available channels[2] and f_1 denote the number of free channels on the link.

The required mapping, $P(T_3, T_4|T_1, T_2)$ is then computed as:

$$P(T_3, T_4|T_1, T_2) = \sum_{f_1=0}^{KS} \sum_{f_2=f_1}^{KS} P(f_1, f_2|T_1, T_2) P(T_3, T_4|T_1, T_2, f_1, f_2) \tag{9}$$

where $P(f_1, f_2|T_1, T_2)$ denotes the probability of f_2 channels being free on the link with f_1 among them being available given that T_2 trunks are free on the link with T_1 among them being available for a path upto that link. $P(T_3, T_4|f_1, f_2)$ denotes the probability of having T_4 free trunks with T_3 among them available as viewed by another node given that f_2 channels are free on the link with f_1 among them being available.

$P(f_1, f_2|T_1, T_2)$ is computed by conditioning on the number of free channels available in the link as:

$$P(f_1, f_2|T_1, T_2) = P(f_2|T_1, T_2)\ P(f_1|T_1, T_2, f_2) \tag{10}$$

$$= P(f_2|T_2)\ P(f_1|T_1, T_2, f_2) \tag{11}$$

where $P(f_2|T_1, T_2)$ denotes the probability of having f_2 channels free in the link given that T_2 trunks are free with T_1 among them being available. This is reduced to $P(f_2|T_2)$ as the number of free channels on the link does not depend on the available trunks in the path. This probability is computed using the two-link model described in [8].

$P(f_1|T_1, T_2, f_2)$ denotes the probability of f_1 channels being available on the link given that T_2 trunks are free with T_1 of them being available and f_2

channels free. It is computed as:

$$P(f_1|T_1, T_2, f_2) = \frac{\xi_{T_1}(f_1)\xi_{T_2-T_1}(f_2 - f_1)}{\sum_{f=0}^{f_2} \xi_{T_1}(f)\xi_{T_2-T_1}(f_2 - f)} \tag{12}$$

where $\xi_t(f)$ denotes the number of ways of arranging f free (or available) channels across t free (or available) trunks such that each trunk has atleast one free (or available) channel in it. It has to be noted that for a trunk to be called free (or available), there has to be at least one free (or available) channel in it. $\xi_t(f)$ is computed as:

$$\xi_T(f) = \sum_{x=1}^{min(S_1,f)} \xi_1(x)\xi_{t-1}(f - x) \tag{13}$$

$\xi_1(x)$ denotes the number of ways of arranging x free channels over a trunk. With S_1 channels per trunk, $\xi_1(x)$ is written as:

$$\xi_1(x) = \begin{cases} \binom{S_1}{x} & \text{if } 1 \leq x \leq S_1 \\ 0 & \text{otherwise.} \end{cases} \tag{14}$$

The probability of finding the trunk distribution as viewed by the second node given the trunk distribution and the channel distribution as viewed by the first node depends on how the channels are distributed across the trunks at the two nodes. While there could be several possible choices, there are two cases that are of interest: (1) only the number of trunks that a link is viewed as is known for both the nodes and the exact architectures are not known; and (2) the precise grooming architecture at the two nodes are known.

Case 1: Architecture independent mapping
In this case, we assume the exact architecture of the two nodes connected to the link are not known. The only information that is known is the number of trunks that each node views the link as. The precise mapping of channels from a trunk as viewed by one node to that viewed by the other is not known. Due to the lack of the exact architecture, the knowledge of the channel distribution alone is employed for mapping the trunk distribution. The required probability, $P(T_3, T_4|T_1, T_2, f_1, f_2)$ is computed as:

$$P(T_3, T_4|T_1, T_2, f_1, f_2) = \begin{cases} \frac{\zeta_{T_4}(T_3, f_1, f_2)}{\sum_{t_3=0}^{K_2}\sum_{t_4=t_3}^{K_2} \zeta_{t_4}(t_3, f_1, f_2)} \\ \qquad \text{if } T_3 \leq T_4 \\ 0 \qquad \text{otherwise} \end{cases} \tag{15}$$

where $\zeta_t(t', f_1, f_2)$ denotes the number of ways of arranging f_2 calls across t trunks such that a trunk having a call belonging to the f_1 available trunk would result in exactly t' trunks being available. This value is computed as:

$$\zeta_t(t', f_1, f_2) = \begin{cases} \frac{t}{t'} \sum_{x=1}^{min(f_1,S_2)} \sum_{y=x}^{min(f_2,S_2)} \\ \quad \zeta_{t-1}(t'-1, u_1 - x, u_2 - y)\zeta_1(1, x, y) \\ \quad \quad \text{if } t' > 0 \text{ and } u_1 > 0 \\ \sum_{y=1}^{min(f_2,S_2)} \zeta_{t-1}(t, f_1, f_2 - y)\zeta_1(1, x, y) \\ \quad \quad \text{if } t' = 0 \text{ and } u_1 = 0 \end{cases} \tag{16}$$

It has to be noted that the computation of the probability $P(T_3, T_4|T_1, T_2, f_1, f_2)$ does not depend on T_1 and T_2.

Case 2: Architecture-dependent mapping

This choice arises from the architectural viewpoint. Note that when a link has multiple fibers, wavelengths and time slots, the alternatives for trunk switching are limited to treating either wavelength or time slot as a trunk, when only limited switching is allowed. In such a case, two nodes that view the link differently would have the channel distribution as considered here. For example, consider a link with two wavelengths and three time slots per wavelength. Let Node 1 view the link as wavelength trunks, i.e., 2 trunks with three channels in each. Let Node 2 view the link as time slot trunks, i.e., 3 trunks with 2 channels in each. This scenario is depicted in Fig. 6 showing the distribution of channels across trunks as seen by the two nodes.

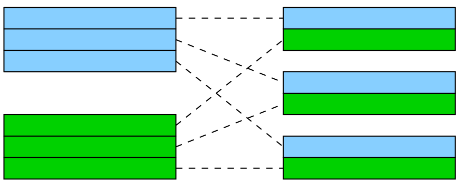

Figure 6. Channel distribution across trunks as viewed by two nodes employing different switching architectures.

In this case, due to the regularity in the channel distribution, the knowledge of the trunk and channel distribution as seen by Node 1 could be used to derive the lower bound on the trunk distribution as seen by Node 2. For example, if three channels are free with one trunk being free as viewed by Node 1, then, the a minimum of three trunks need to be free as viewed by Node 2. In general, if f_1 channels and T_1 ($f_1 > 0$ and $T_1 > 0$) trunks are free, then a minimum of $\frac{f_1 K_2}{T_1 S_1}$ trunks must be free as viewed by the second node. Recall that, K_2 denotes the total number of trunks in a link as viewed by Node 2 and S_1 denotes the number of channels per trunk as viewed by Node 1. The same reasoning is true for the lower bound on the available trunks as well.

The required probability $P(T_3, T_4 | T_1, T_2, f_1, f_2)$ is then computed by setting the probability values of those trunk distributions that are not feasible to zero, specifically $P_(T_3, T_4 | T_1, T_2, f_1, f_2)$ is set to 0 if one of the following holds true.

$$T_1 > 0 \text{ and } T_3 < \frac{f_1 K_2}{T_1 S_1} \tag{17}$$

$$T_2 > 0 \text{ and } T_4 < \frac{f_2 K_2}{T_2 S_1} \tag{18}$$

The probabilities are then normalized to obtain the sum of all the conditional probabilities to 1. These pruning of state-space depends entirely on the architecture, hence will be different for different architectures.

4. Simulation of WDM grooming networks

In order to simulate a WDM grooming network for blocking performance, nodes with different grooming capabilities need to be simulated. We employ the MICRON (Methodology for Information Collection and Routing in Optical Networks) framework, developed in [9], for connection establishment in WDM grooming network. The MICRON framework presents a matrix-based methodology to store link information, combines the link information to obtain path information using generalized matrix multiplication, and provides a generic methodology for sub-trunk assignment on a chosen path. We briefly describe the MICRON framework with an example as applied to the network model considered in this paper.

4.1. Example network

Consider the example two paths from Node 1 to 5 in a network shown in Fig. 7. Let the nodes be connected using 3 fibers each carrying 3 wavelengths and 2 time slots per wavelength. Also assume that nodes 1, 3, 6, and 7 are wavelength-level grooming nodes; nodes 2 and 5 are time-slot-level grooming nodes; and node 4 is a full-grooming node. Wavelength-level grooming nodes view the link as 3 wavelength trunks (denoted by W_1, W_2, and W_3) with 6 channels in each, time slot-level grooming nodes view a link as two time slot trunks (denoted by T_1 and T_2) with 9 channels in each, and a full-grooming node views a link as one trunk (denoted by F_1) with 18 channels.

Fig. 8 shows the expanded view of the network indicating the different trunks at the nodes. For example, consider trunk W1 of Node 1 and trunk T1

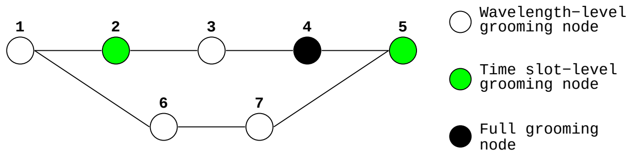

Figure 7. An example network showing two paths from node 1 to node 5.

of Node 2. The number of channels in the link 1–2 (denoted by $\ell_1 2$) that belongs to both the trunks is 3. The channels are $(\ell_{12}, 1, 1, 1)$, $(\ell_{12}, 2, 1, 1)$ and $(\ell_{12}, 3, 1, 1)$, each channel belonging to a distinct fiber. The arrow connecting trunk W1 of Node 1 to trunk T1 of Node 2 indicates the number of free channels that belong to both the trunk definitions. A value of 3 indicates that all the channels belonging to both the trunk definitions are free.

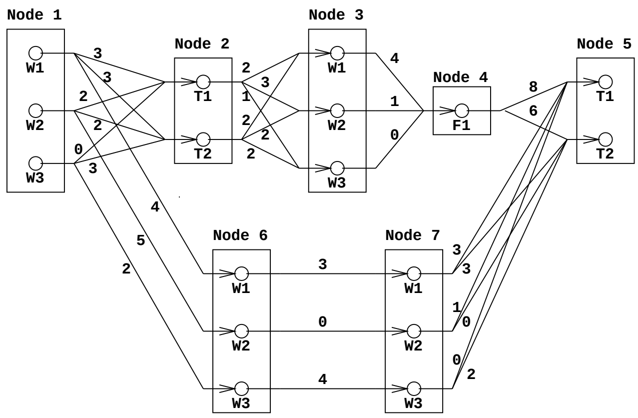

Figure 8. Expanded view of the network with channel occupancy information

Assume that the network is observed at some instant of time during its operation and the channel occupancy in the links are known. Let $(l, f, w, t).Availability$ denote the availability of the channel: denoted by 0 if occupied by a connection, 1 if the channel is free.

4.2. Link information

A link connecting Node i and j is represented by a matrix L_{ij}.

$$L_{ij} = \begin{bmatrix} l_{11} & l_{12} & ... & l_{1K_j} \\ l_{21} & l_{22} & ... & l_{2K_j} \\ . & & & \\ . & & & \\ l_{K_i1} & l_{K_i2} & ... & l_{K_iK_j} \end{bmatrix} \quad (19)$$

where each element l_{xy} denotes a certain property about the channels in the link that belong to sub-trunk Θ_{xy}^{ij}. For example, consider the Link 1–2 in the example network shown in Fig. 7. Node 1 views each wavelength as a trunk, hence has 3 trunks. Node 2 views each time slot as a trunk, hence has 2 trunks. Hence, L_{12} is a 3×2-matrix.

The matrix can denote different properties of the channels. For the simulations considered in this paper, we employ the information about the channel availability to route connections requiring one channel capacity. Every element l_{xy} of the matrix L_{ij} is denoted by 1 if the total number of free channels that belong to Θ_{xy}^{ij} has a capacity of at least B. The matrix L_{ij} is defined as:

$$l_{xy} = \begin{cases} 1 & \text{if } \left(\sum_{(l,f,w,t)\in\Theta_{xy}^{ij}} (l,f,w,t).Availability\right) > 0 \\ 0 & \text{otherwise} \end{cases} \quad (20)$$

where $1 \leq x \leq K_i$ and $1 \leq y \leq K_j$. The matrices indicating the connectivity information for different links are shown in Fig. 9.

$$L_{12} = \begin{bmatrix} 1 & 1 \\ 1 & 1 \\ 0 & 1 \end{bmatrix} \quad L_{23} = \begin{bmatrix} 1 & 1 & 1 \\ 1 & 1 & 1 \end{bmatrix} \quad L_{34} = \begin{bmatrix} 1 \\ 1 \\ 0 \end{bmatrix} \quad L_{45} = \begin{bmatrix} 1 & 1 \end{bmatrix}$$

$$L_{16} = \begin{bmatrix} 1 & 0 & 0 \\ 0 & 1 & 0 \\ 0 & 0 & 1 \end{bmatrix} \quad L_{67} = \begin{bmatrix} 1 & 0 & 0 \\ 0 & 0 & 0 \\ 0 & 0 & 1 \end{bmatrix} \quad L_{75} = \begin{bmatrix} 1 & 1 \\ 1 & 0 \\ 0 & 1 \end{bmatrix}$$

Figure 9. Link information matrices indicating if there is at least one free channel in a sub-trunk.

4.3. Path information

The information about a certain path from a Node i to k that are not physically connected by a fiber can be obtained by combining the link information in the path. The matrix representation for a path is defined in a manner similar to that of a link. A path matrix from node i to k through j is obtained as a matrix multiplication of individual path segments P_{ij} and P_{jk} as:

$$P_{ik} = P_{ij}P_{jk} \quad (21)$$

We employ a generalized version of matrix multiplication to compute the path metric. An element p_{xy}^{ik} (the superscript ik denotes the matrix to which the element belongs to) is obtained as:

$$p_{xy}^{ik} = (p_{x1}^{ij} \otimes p_{1y}^{jk}) \oplus (p_{x2}^{ij} \otimes p_{2y}^{jk}) \oplus ... \oplus (p_{xK_j}^{ij} \otimes p_{K_j y}^{jk}) \qquad (22)$$

The operators $\otimes$ and $\oplus$, denoted as a tuple $(\otimes, \oplus)$, can be defined in different combinations so that several meaningful results are obtained. It can be observed that when $\otimes$ is integer multiplication and $\oplus$ is integer operation, the above equation denotes the traditional matrix multiplication.

In this paper, we assume that all the requests are for a single channel capacity. Hence, it is sufficient to identify if there is a connectivity from source to destination. To achieve this, we choose the *selection operator* (min, max).

Applying this set of operation to the matrix representation in Fig. 9, we obtain the matrix representation for the path 1–2–3–4–5 as:

$$P_{1-2-3-4-5} = \begin{bmatrix} 1 & 1 \\ 1 & 1 \\ 1 & 1 \end{bmatrix} \qquad (23)$$

The elements of the matrix indicate the existence of a sub-trunk assignment scheme for one channel capacity call that would start at trunk x at Node 1 and end at trunk y at Node 5. The existence of these possible trunk assignments can be easily verified from Fig. 8.

With this information, the destination node first chooses the trunk at which the connection would end. Given that the trunk assignment at the destination is chosen, the sub-trunk assignment on the link or the trunk assignment at the previous node is chosen as one of the possible trunks that would result in the termination of the connection at the chosen trunk in the destination. This procedure is iterated until a trunk assignment at the source is found. For detailed procedure on sub-trunk assignment on links or trunk assignment at nodes, the readers are referred to [7].

Once the sub-trunk assignment has been made, any free channel belonging to the sub-trunk assigned at a link can be chosen for establishing the channel as every node has full-permutation switching capability within a trunk.

5. Performance evaluation

We consider a 9-node uni-directional ring and 3×3 uni-directional mesh-torus mesh-torus networks with three types of nodes (or grooming capabilities) for evaluating the blocking performance. These networks are shown in Fig. 10. The choice of these two regular networks are due to the high and the low correlation values for ring and mesh-torus network, thus verifying the analytical model for a wide range of networks.

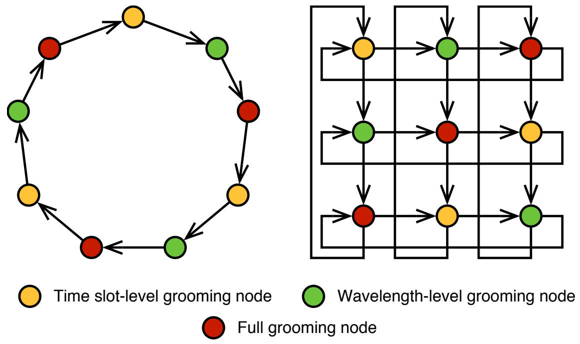

Figure 10. A 9-node heterogeneous uni-directional ring and 9-node heterogeneous uni-directional mesh-torus networks with three different switch architectures.

It can be seen that any path with a certain path length can be classified into three categories depending on the source. We refer to a path originating from a time-slot level grooming node as Path-1, wavelength-level grooming node as Path-2, and full-grooming node as Path-3.

We consider a link with 20 channels organized as two fibers, five wavelengths per fiber, and two time slots per wavelength. We assume that all calls have a requirement of one time slot capacity. The results of the analytical model to be shown in the graphs are obtained without employing the knowledge about the trunk distribution for mapping the trunk distribution between adjacent nodes.

Figs. 11 shows the blocking performance of a 9-node uni-directional ring network with nodes employing full-permutation switching in each trunk for three different path types with varying path lengths for offered network load of 15 and 21 Erlangs (link loads of 7.5 and 10.5 rlangs).

It is observed that the performance trend observed with the simulation for the different path lengths is also observed through the analysis. The blocking performance as estimated by the analysis is the same for all the paths with a length of one hop. This is due to the reason that a single hop blocking performance remains the same for a given link load and correlation factor for any switch architecture. For two-hop paths, the blocking performance depends on the switching capability of intermediate node. Calls that would have the intermediate node as a full grooming node (Path-2) would experience the least blocking while calls with intermediate node as a wavelength-level grooming node (Path-1) would have the highest blocking among calls that require two-hop connections. Similarly, for three-hop connections, calls with intermediate nodes as FG and TG nodes (Path-2) would experience lowest blocking while calls with TG and WG nodes as intermediate nodes (Path-3) would experience the maximum blocking. Now, note that as more calls requiring connections

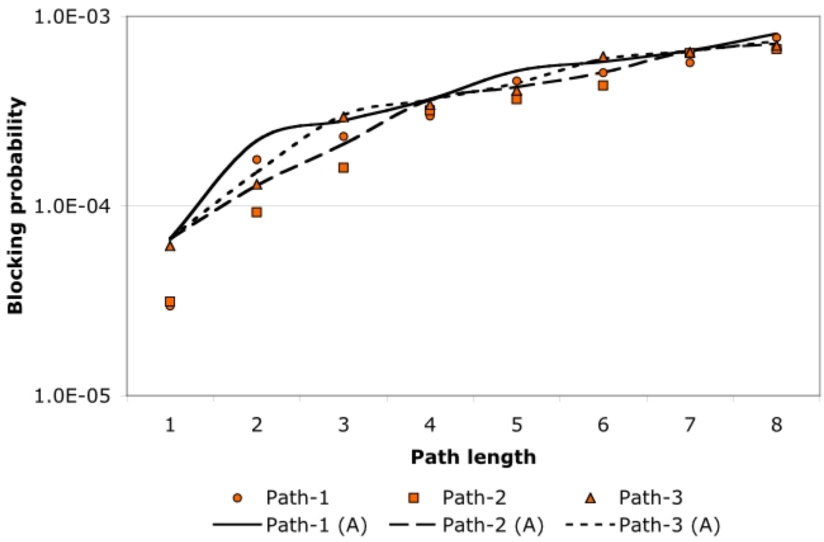

(a)

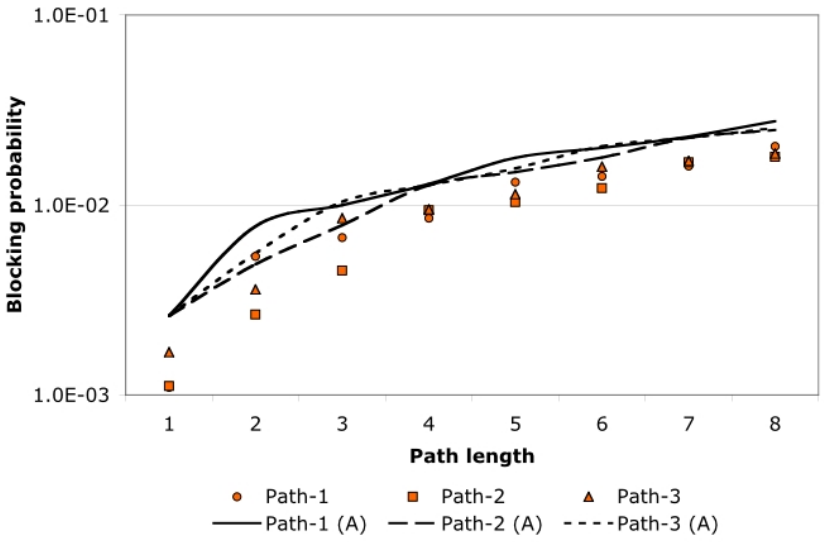

(b)

Figure 11. Blocking performance of 9-node heterogeneous uni-directional ring network with nodes employing full-permutation switching in each trunk for varying network loads. (a) 15 Erlangs and (b) 21 Erlangs.

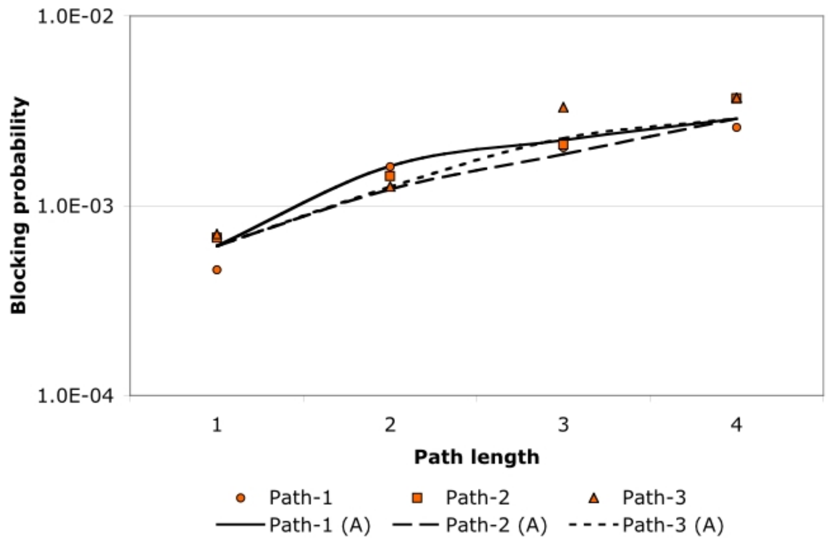

(a)

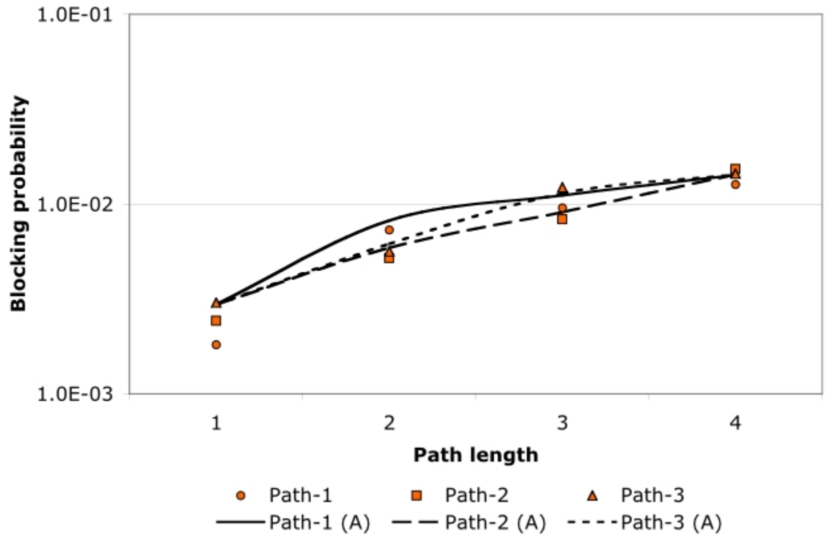

(b)

Figure 12. Blocking performance of 3×3 heterogeneous uni-directional mesh-torus network with nodes employing full-permutation switching in each trunk for varying network loads. (a) 72 Erlangs and (b) 84 Erlangs.

for two and three hops will be rejected at a wavelength-level grooming node due to the insufficient switching capacity at the immediate neighboring node, calls requiring one-hop connection originating at the WG node would experience lesser blocking performance. It is observed that these performance trends remain the same with the increasing load, thus depending only on where the nodes are positioned. It is to be noted that although the analytical model shows these trends, the difference in blocking performance between calls of different categories are not exactly the same as seen in the simulation results. Hence, minor differences in the blocking probabilities seen through simulations may not be observed through analytical model.

Figs. 12 show sthe blocking performance for paths originating at different nodes versus the path length for offered network loads of 72 and 84 Erlangs (link loads of 9 and 10.5 Erlangs) in a 3×3 heterogeneous uni-directional mesh-torus network with nodes employing full-permutation switching in every trunk. It is observed that the performance trends exhibited by the simulation is also reflected by the analytical prediction, although the difference in blocking performance as predicted by simulation and analysis are different.

As the network load increases, the accuracy of the analytical model drops. Such a trend is pronounced in ring networks due to longer average path length. In order to improve the accuracy of the model, iterative mechanisms that adjust the network load and link correlation as described in [7] can be employed.

The difference in blocking performance obtained using the analytical model with and without the exact knowledge on the architectures of nodes was found to be less than 2%. Hence, these results are not in the paper explicitly. While this has been verified for the grooming architectures considered in this paper, further analysis and simulations are required to validate the same for other grooming architectures. The analytical model presented in this paper can be employed by resource placement algorithms that identify a set of nodes that needs to be upgraded when resources are limited, for example, placing a few wavelength converter nodes in a network as considered in [11].

6. Conclusion

In this paper, we develop an analytical model for evaluating the blocking performance of WDM grooming networks employing heterogeneous grooming architectures. The analytical model assumes fixed-path routing and unit call capacity requirement for the traffic. We show through comparisons with simulations results, that the analytical model accurately predicts the blocking performance of path involving nodes with different grooming architectures. We observe that the results of the analytical model with and without the precise knowledge on the grooming architectures do not differ by more than 2%.

We believe that the analytical model will find application in situation where a set of nodes need to be identified for upgrading when resources are limited.

Notes

1. The destination is not considered as the last node in the path.
2. Available channels are those free channels in the set of available trunks.

References

[1] Barry, R. and P. Humblet: 1996, 'Models of blocking probability in all-optical networks with and without wavelength changers'. *IEEE Journal of Selected Areas in Communications* **14**(5), 858–867.

[2] Birman, A.: 1995, 'Computing approximate blocking probabilities for a class of all-optical networks'. In: *Proceedings of IEEE INFOCOM'95*. pp. 651–658.

[3] Kovacevic, M. and S. Acampora: 1996, 'Benefits of wavelength translation in all-optical clear-channel networks'. *IEEE Journal of Selected Areas in Communications* **14**(5), 868–880.

[4] Lee, K. C. and V. O. K. Li: 1993, 'A wavelength-convertible optical network'. *Journal of Lightwave Technology* **11**(5), 962–970.

[5] Li, L. and A. Somani: 1999, 'A new analytical model for multi-fiber WDM networks'. In: *Proceedings of the Global Telecommunications Conference, GLOBECOM'99*, Vol. 1B. pp. 1007–1011.

[6] Ramaswami, R. and G. Sasaki: 1998, 'Multiwavelength optical networks with limited wavelength conversion'. *IEEE/ACM Transactions on Networking* **6**(6), 744–754.

[7] Srinivasan, R.: 2002, 'A generalized framework for analyzing time-space switched optical networks'. *PhD Dissertation, Iowa State University*.

[8] Srinivasan, R. and A. K. Somani: 2002, 'A generalized framework for analyzing time-space switched optical networks'. *IEEE Journal of Selected Areas in Communications: Special Issue on WDM-based Network Architectures* pp. 202–215.

[9] Srinivasan, R. and A. K. Somani: 2003, 'MICRON – A framework for connection establishment in optical networks'. *submitted to IEEE INFOCOM*.

[10] Subramaniam, S., M. Azizoglu, and A. Somani: 1996, 'All-optical networks with sparse-wavelength conversion'. *IEEE/ACM Transactions on Networking* **4**(4), 544–557.

[11] Thiagarajan, S. and A. K. Somani: 1999, 'An efficient algorithm for optimal wavelength converter placement on wavelength-routed networks with arbitrary topologies'. In: *Proceedings of IEEE INFOCOM'99*.

[12] Tripathi, T. and K. Sivarajan: 1999, 'Computing approximate blocking probabilities in wavelength-routed all-optical networks with limited-range wavelength conversion'. In: *Proceedings of IEEE INFOCOM'99*, Vol. 1. pp. 329–336.

[13] Wauters, N. and P. Demeester: 1997, 'Wavelength conversion in optical multi-wavelength multi-fiber transport networks'. *International Journal of Optoelectronics* **11**(1), 53–70.

[14] Yates, J., J. Lacey, and D. Everitt: 1996, 'Blocking in multiwavelength TDM networks'. In: *4th International Conference on Telecommunication Systems, Modeling, and Analysis*. Nashville, Tennessee, USA, pp. 535–541.